



地球物理与空间信息学院
School of Geophysics and Geomatics

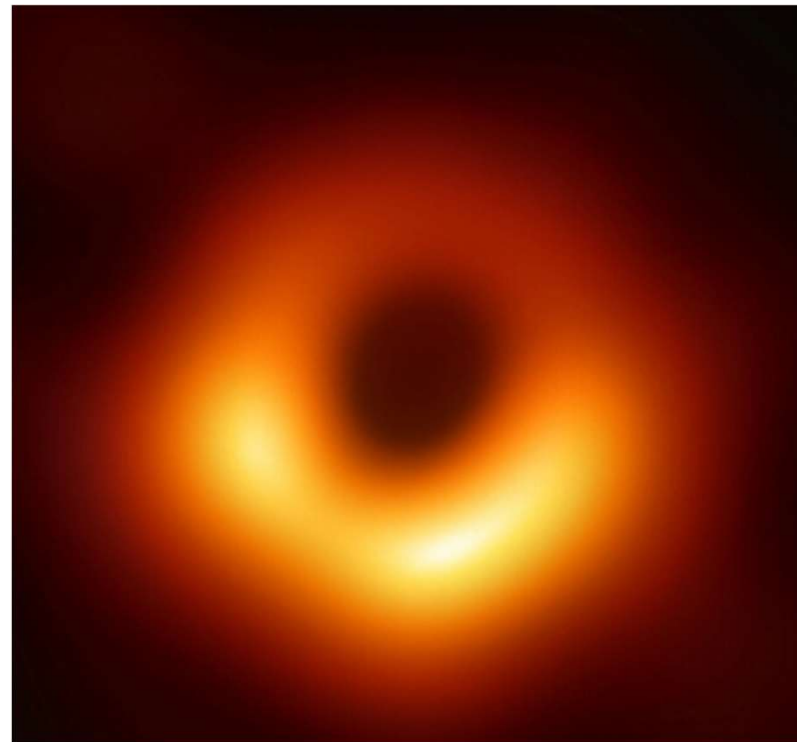
带有薄吸积盘的高阶导数引力球对称黑洞的光学外观

合作人：崔宇昊、郭森、黄宇翔

指导老师：林恺

时间：2023年12月2日

In 2019, the Event Horizon Telescope (EHT) collaboration reported the images of the supermassive BH at the center of the M87* galaxy





- 高阶导数引力理论下的球对称黑洞解
- 黑洞时空中的测地线
- 吸积盘的光线追踪与辐射通量
- 总结

二、高阶导数引力理论下的球对称黑洞解

The most general Lagrangean with quadratic curvature invariants

$$\mathcal{L} = \gamma R - \alpha C_{\mu\nu\rho\sigma} C^{\mu\nu\rho\sigma} + \beta R^2$$

$$\beta = 0 \quad \gamma = 1$$

Einstein field equations

$$R_{\mu\nu} - \frac{1}{2} g_{\mu\nu} - 4\alpha B_{\mu\nu} = 0$$

$$B_{\mu\nu} = \left(\nabla^\rho \nabla^\sigma + \frac{1}{2} R^{\rho\sigma} \right) C_{\mu\rho\nu\sigma}$$

H. Lu, A. Perkins, C.N. Pope, K.S. Stelle, Phys. Rev. Lett. 114, 171601 (2015).

二、高阶导数引力理论下的球对称黑洞解

metric $ds^2 = -h(r)dt^2 + \frac{1}{f(r)}dr^2 + r^2d\theta^2 + r^2\sin^2\theta d\varphi^2$

Field equations

$$rh[rh'f' + 2f(rh'' + 2h')] + 4h^2(rf' + f - 1) - r^2fh'^2 = 0$$

$$f'' + \frac{r^2fh'^2 + 2fhh' + 4(f-1)h^2}{2rfh(rh' - 2h)}f' - \frac{3hf'^2}{4fh - 2rfh'} + \\ \frac{r^3fh' + (r^2f - r^2)h}{\alpha r^2f(rh' - 2h)} + \frac{r^3fh'^3 - 3r^2fhh'^2 - 8(f-1)h^3}{2r^2h^2(rh' - 2h)} = 0$$

consider a linear approximation for $f(r), h(r)$

$$f(r) = 1 - \frac{2M}{r} - e^{-\frac{r}{\sqrt{2}\alpha}}C_1 \left(\frac{1}{8\alpha} + \frac{1}{4\sqrt{2}\alpha r} \right)$$

$$h(r) = h_c \left(1 - \frac{2M}{r} - e^{-\frac{r}{\sqrt{2}\alpha}} \left(\frac{C_1}{2\sqrt{2}\alpha r} \right) \right)$$

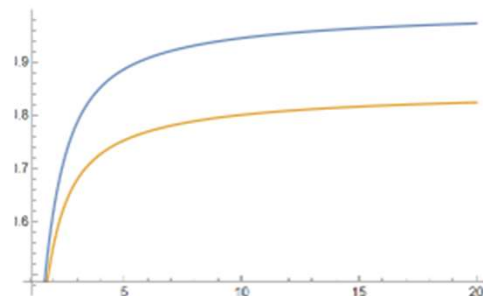
二、高阶导数引力理论下的球对称黑洞解

suppose that the spacetime has only one horizon at r_0

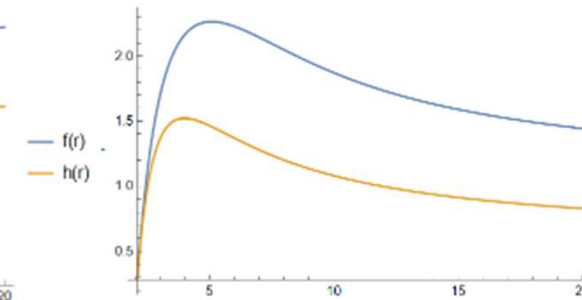
$$h(r) = h_1(r - r_0) + h_2(r - r_0)^2 + h_3(r - r_0)^3 + \dots$$

$$f(r) = f_1(r - r_0) + f_2(r - r_0)^2 + f_3(r - r_0)^3 + \dots$$

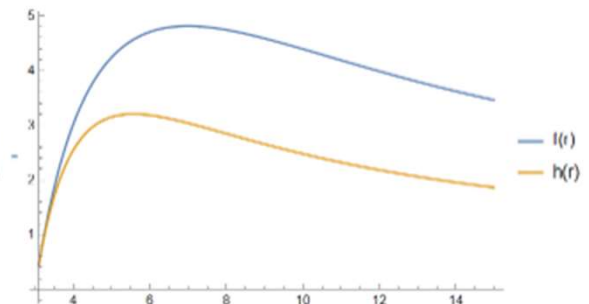
Set $h_1 = f_1$, $\alpha = 1/2$, all h_j and f_j with $j \geq 2$ can be calculated from f_1 .



$$r_0 = 1$$



$$r_0 = 2$$



$$r_0 = 3$$



- 高阶导数引力理论下的球对称黑洞解
- 黑洞时空中的测地线
- 薄吸积盘的辐射通量
- 结论

二、黑洞时空中的测地线

Geodesic equation $-\kappa = g_{\mu\nu} \frac{dx^\mu}{d\lambda} \frac{dx^\nu}{d\lambda}$

$$-\kappa = -\frac{E^2}{h} + \frac{\dot{r}^2}{f} + \frac{L^2}{r^2} \quad E = h(r)\dot{t} \quad L = r^2\dot{\phi}$$

For time-like geodesics $\kappa = 1$

$$\dot{r}^2 = f(r)\left(\frac{E^2}{h(r)} - \frac{L^2}{r^2} - 1\right) \equiv V(r) \quad \ddot{r} = \frac{1}{2}V'(r)$$

circular orbit $\dot{r} = 0 \quad \ddot{r} = 0$

$$E^2 = \frac{2h(r)^2}{2h(r) - rh'(r)} \quad L^2 = \frac{r^3h'(r)}{2h(r) - rh'(r)}$$

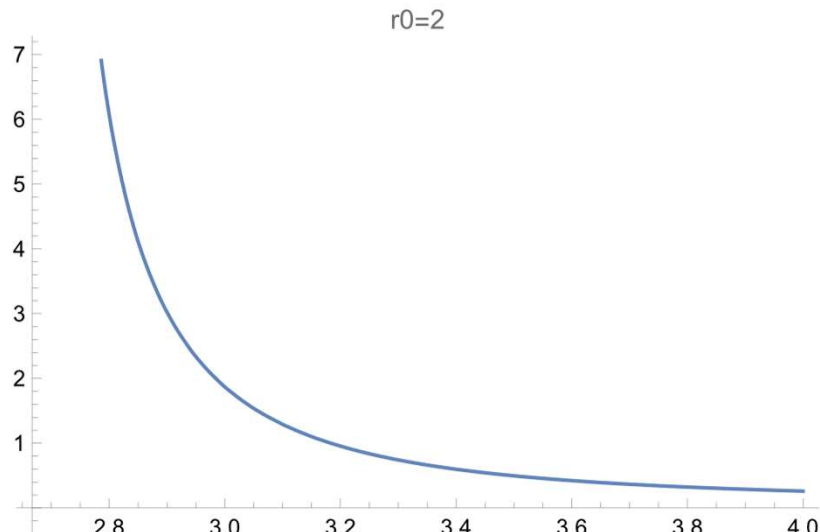
$$2h - rh' > 0 \quad h' > 0$$

$$r > 1.438 \quad 2.666 < r < 3.996 \quad 3.959 < r < 4.572$$

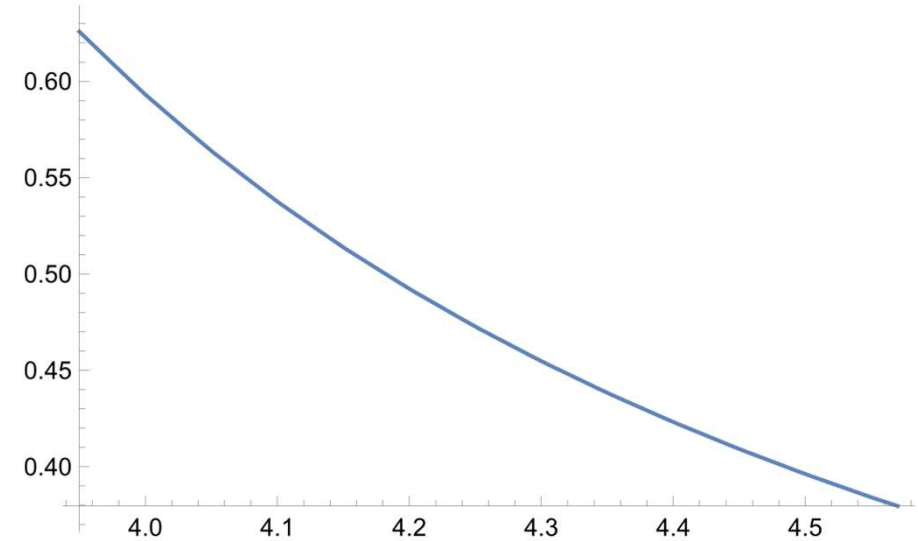
二、黑洞时空中的测地线

The stability of the orbit requires $V''(r) < 0$

$$r_0 = 1 \quad r_{isco} = 3.50201$$



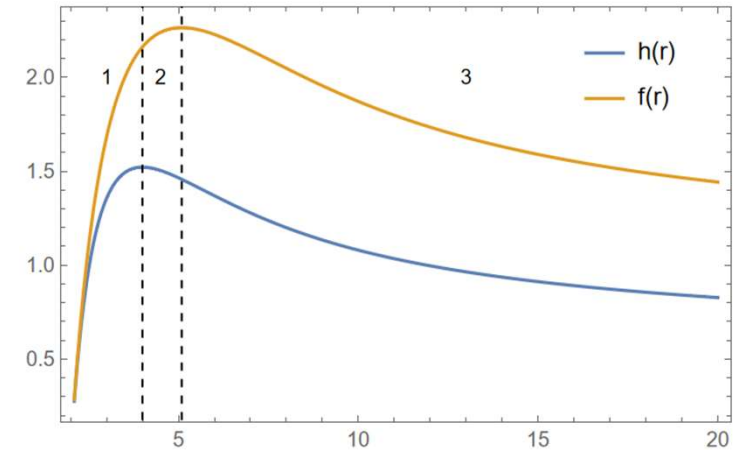
$$r_0 = 2$$



$$r_0 = 3$$

二、黑洞时空中的测地线

$$\ddot{r} = \frac{1}{2} \left[\left(\frac{E^2}{h} - \frac{L^2}{r^2} - 1 \right) f' + f \left(\frac{2L^2}{r^3} - \frac{E^2 h'}{h^2} \right) \right]$$

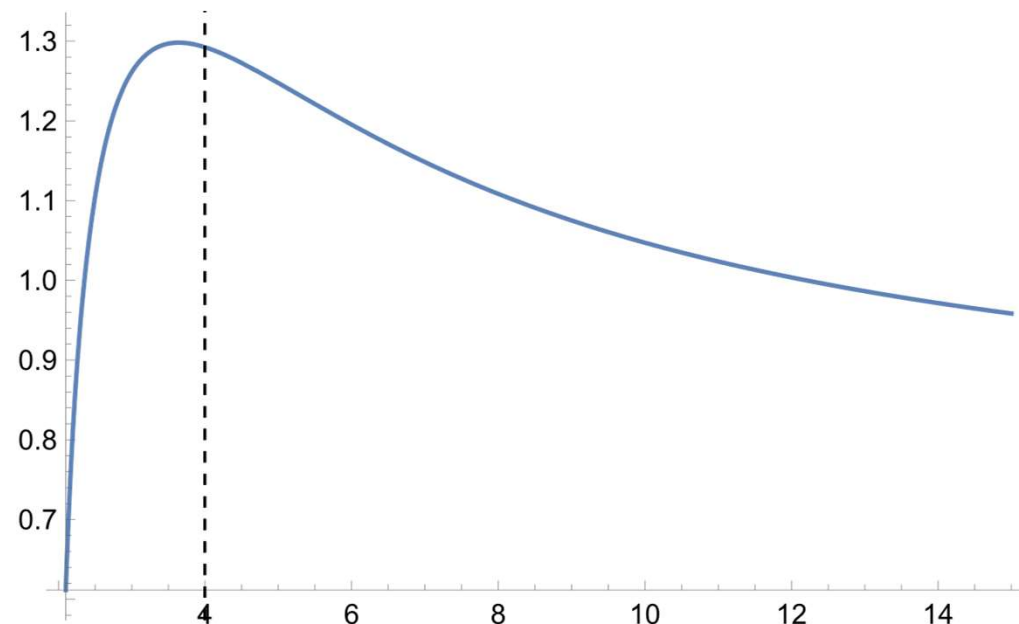
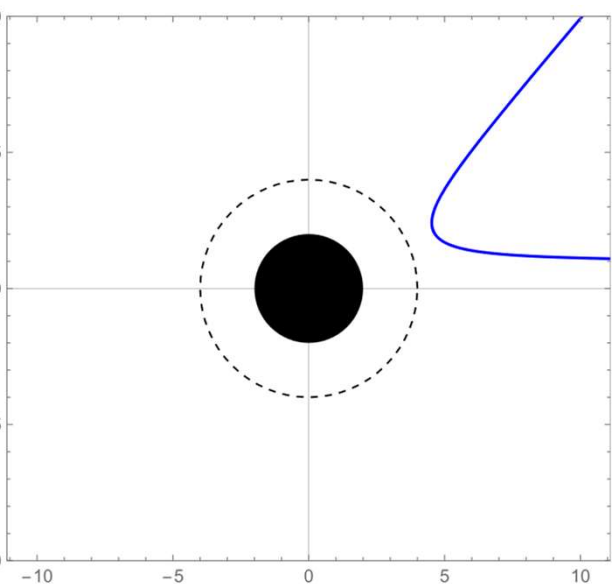
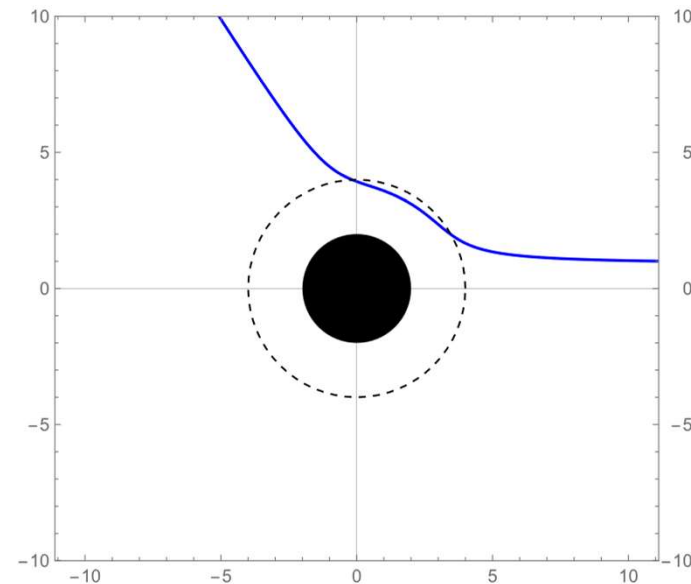
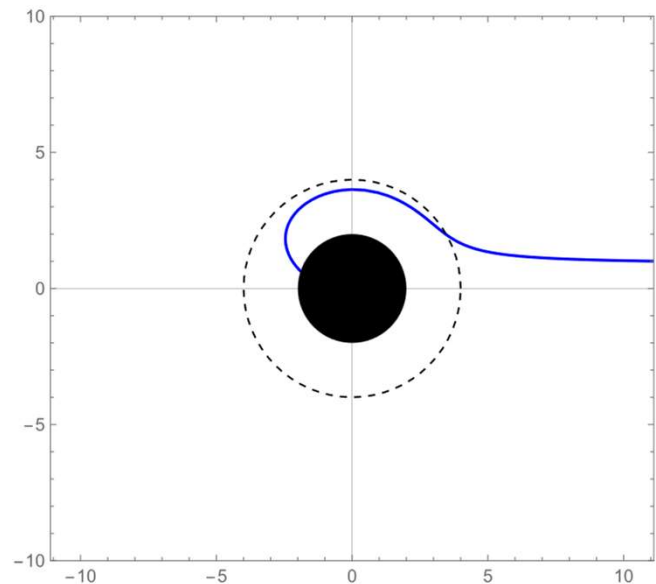


For any E,L

$$\ddot{r} = \frac{2L^2 f}{r^3} - \frac{L^2 f'}{r^2} - f' + E^2 \left(\frac{f'}{h} - \frac{f h'}{h^2} \right)$$

$$h f' - f h' > 0$$

二、黑洞时空中的测地线



$$L=1.25$$

二、黑洞时空中的测地线

Null geodesic $0 = g_{\mu\nu} \frac{dx^\mu}{d\lambda} \frac{dx^\nu}{d\lambda}$

Orbital equation

$$\left(\frac{dr}{d\varphi} \right)^2 = r^4 f(r) \left(\frac{1}{b^2 h(r)} - \frac{1}{r^2} \right) \quad b = \frac{L}{E}$$

The circular orbit of photons

$$r_s = 1.437 \quad b_s = 2.357$$

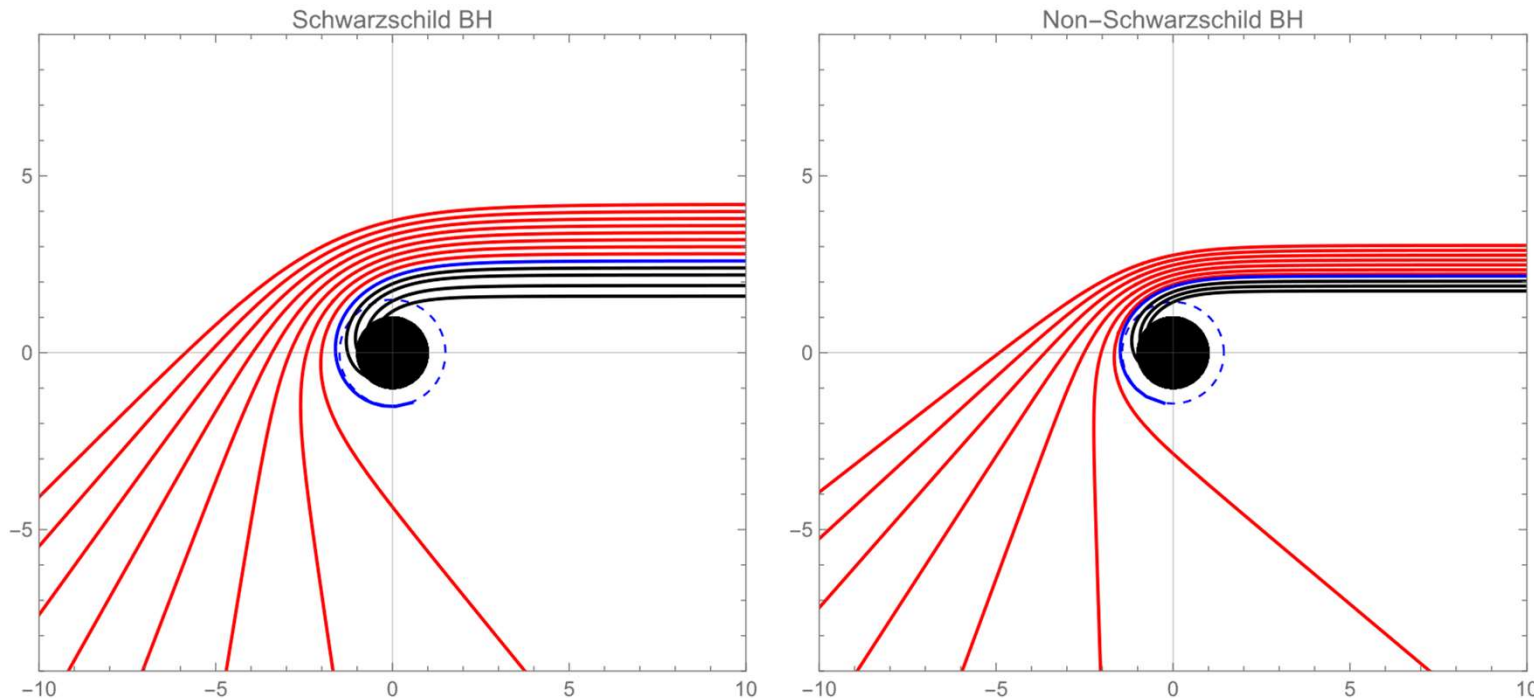
The deflection angle of photons

$$\gamma = \int_{r_{source}}^{\infty} \frac{dr}{\sqrt{r^4 f(r) \left(\frac{1}{b^2 h(r)} - \frac{1}{r^2} \right)}}$$

二、黑洞时空中的测地线

The deflection angle of photons passing through perihelion

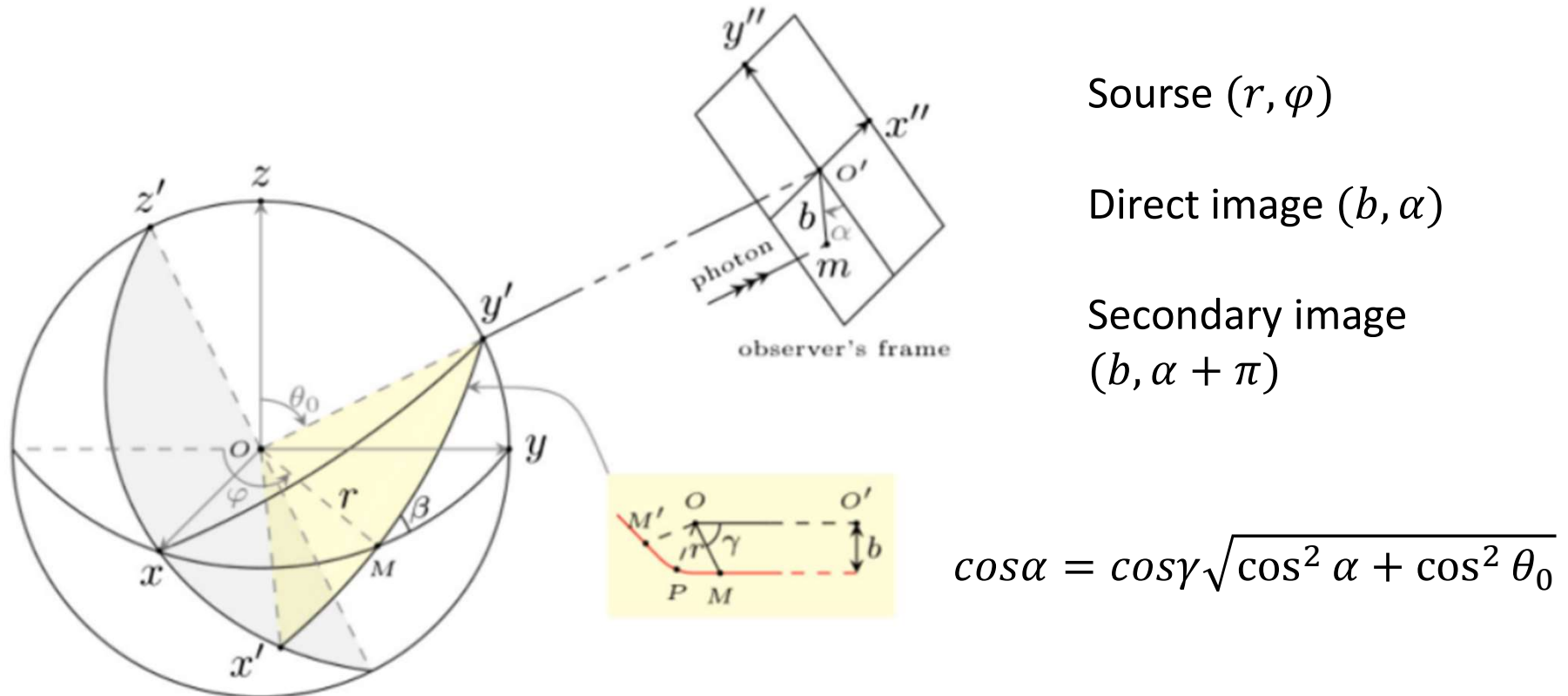
$$\gamma_1 = 2 \int_{r_p}^{\infty} \frac{dr}{\sqrt{r^4 f(r) \left(\frac{1}{b^2 h(r)} - \frac{1}{r^2} \right)}} - \gamma$$





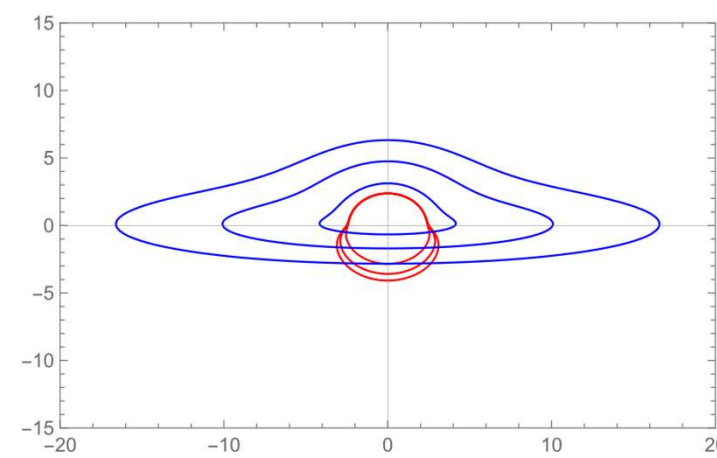
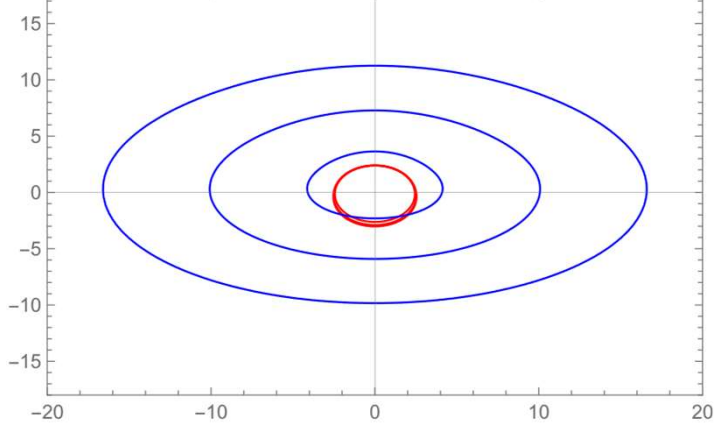
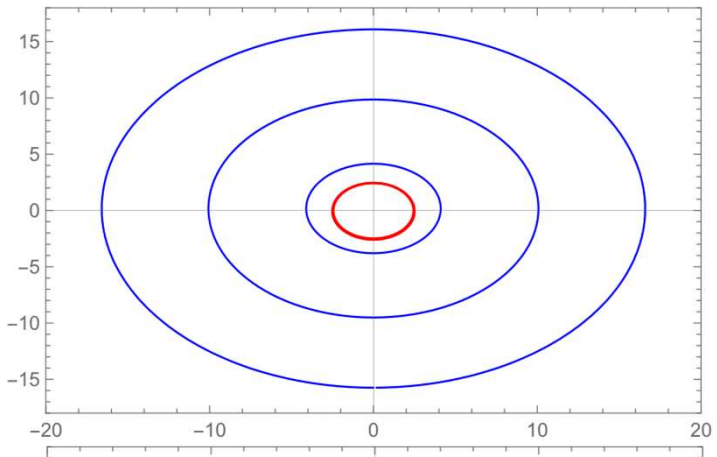
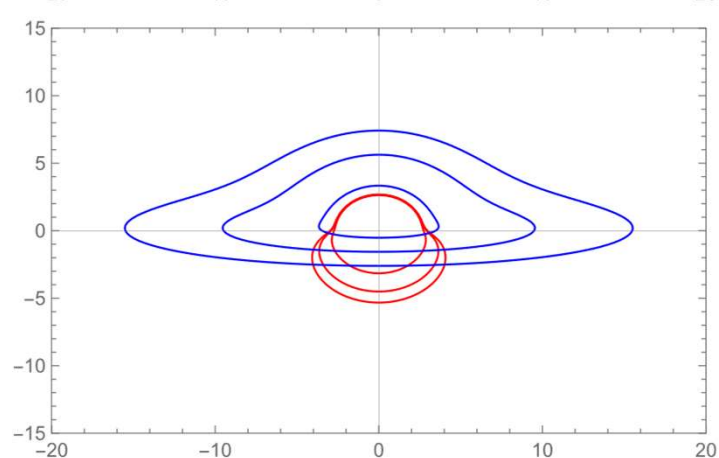
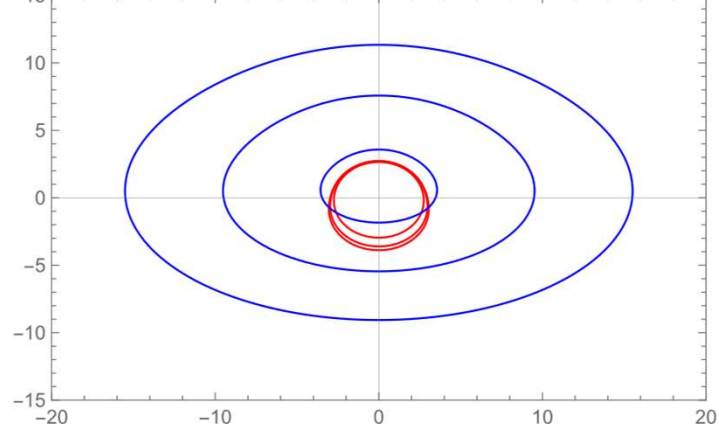
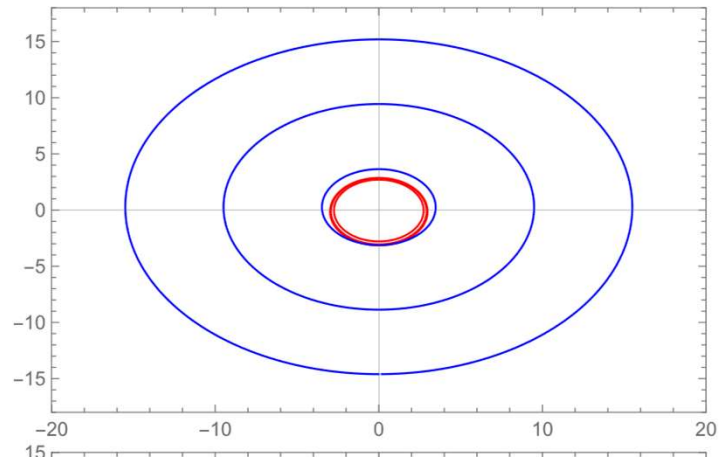
- 高阶导数引力理论下的球对称黑洞解
- 黑洞时空中的测地线与光线追踪
- 吸积盘的光线追踪与辐射通量
- 结论

二、黑洞时空中的测地线



J.-P. Luminet, Image of a spherical black hole with thin accretion disk, Astron. Astrophys. 75, 1 (1979).

二、黑洞时空中的测地线

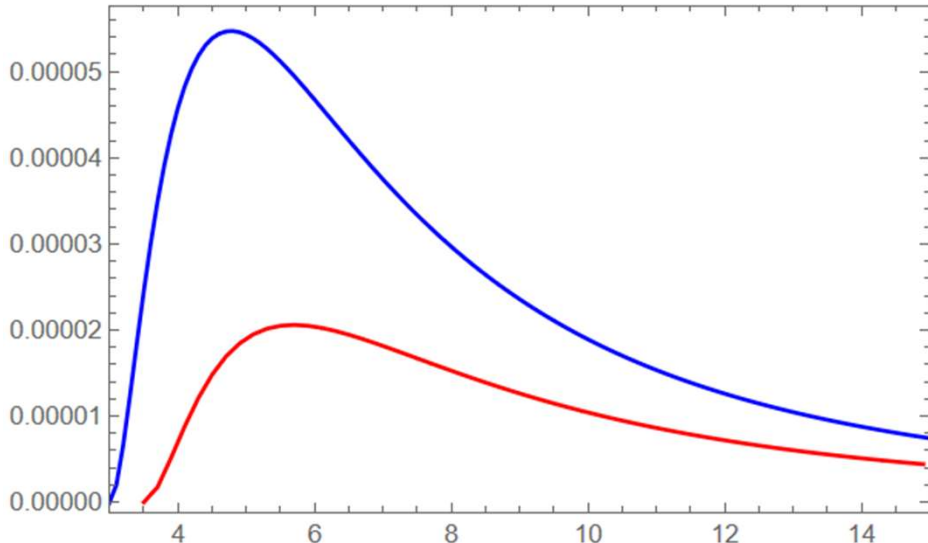


三、吸积盘的光线追踪与辐射通量

The expression of radiation flux of a Novikov-Thorne thin accretion disk

$$F = -\frac{\dot{M}}{2\pi\sqrt{-g}} \frac{\Omega_{,r}}{(E - \Omega L)^2} \int_{r_{in}}^r (E - \Omega L) L_{,r} dr$$

$$E = -\frac{g_{tt}}{\sqrt{-g_{tt} - g_{\varphi\varphi}\Omega^2}} \quad L = -\frac{g_{\varphi\varphi}\Omega}{\sqrt{-g_{tt} - g_{\varphi\varphi}\Omega^2}} \quad \Omega = \frac{d\varphi}{dt} = -\sqrt{-\frac{g_{tt,r}}{g_{\varphi\varphi,r}}}$$



$$F_{max} = 5.471 \times 10^{-5} \cdot \dot{M}$$

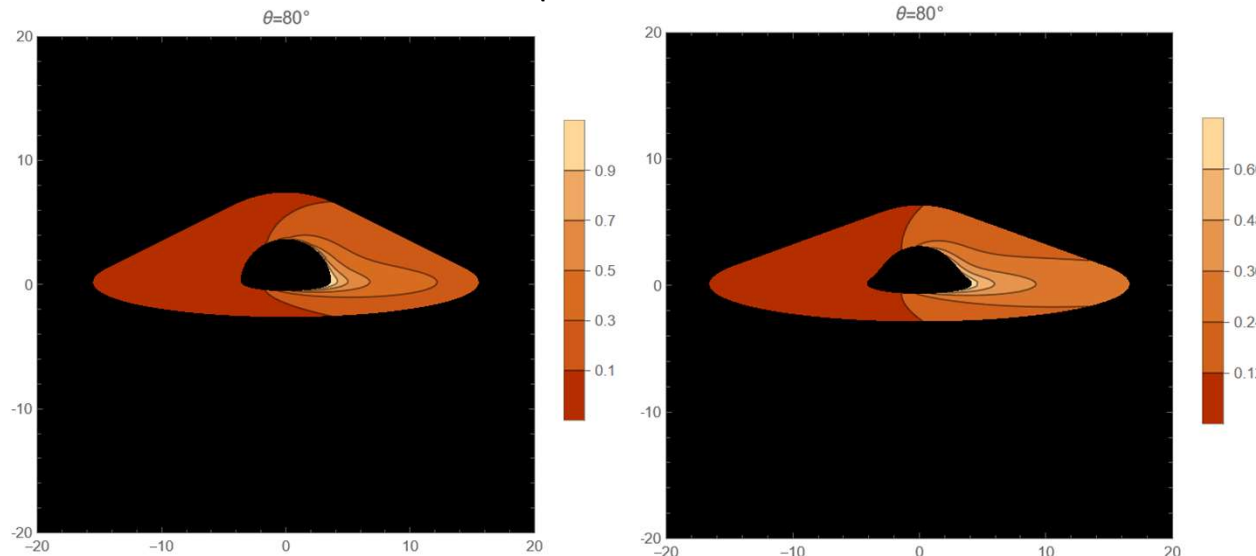
三、吸积盘的光线追踪与辐射通量

Gravitational redshift and Doppler shift can affect the radiative flux

$$F_{obs} = \frac{F}{(z + 1)^4}$$

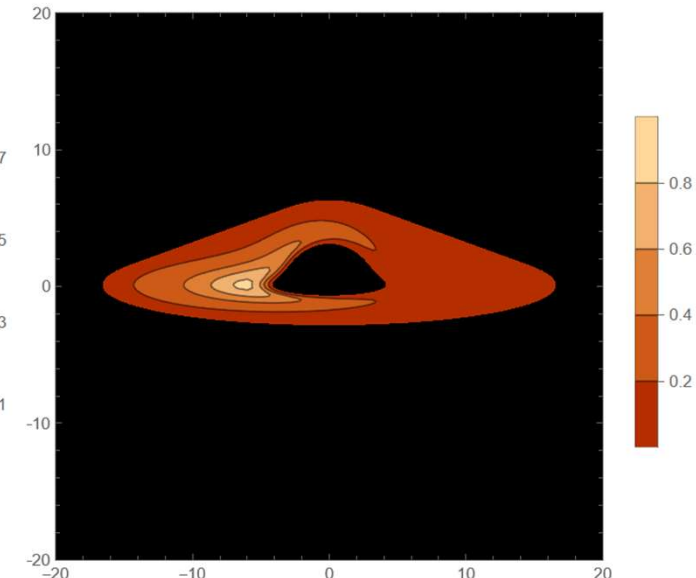
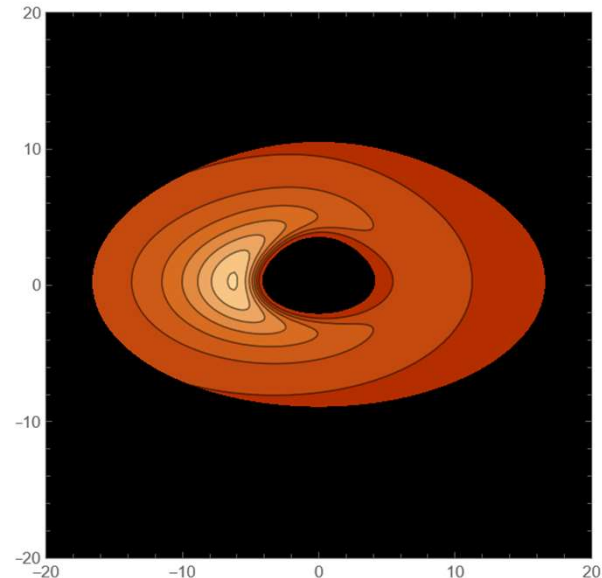
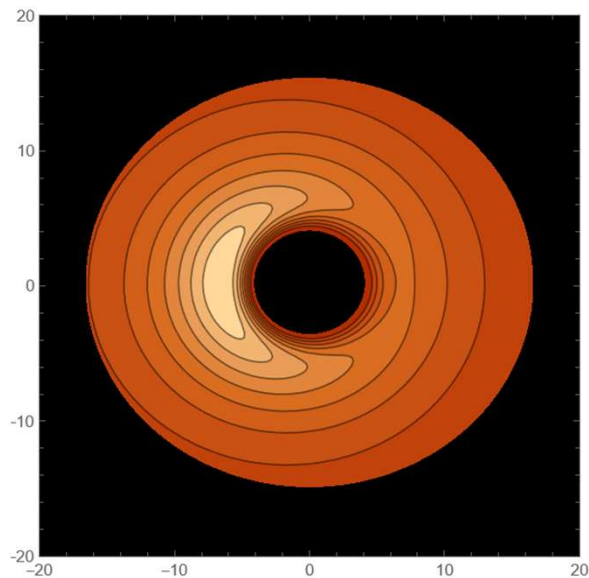
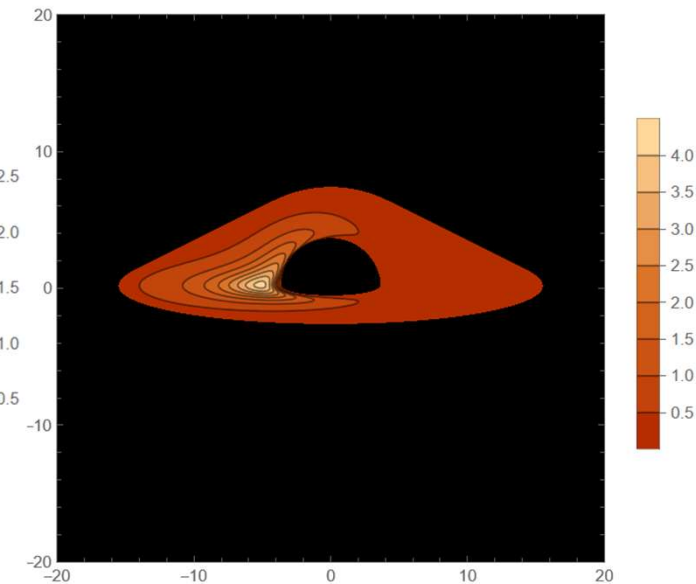
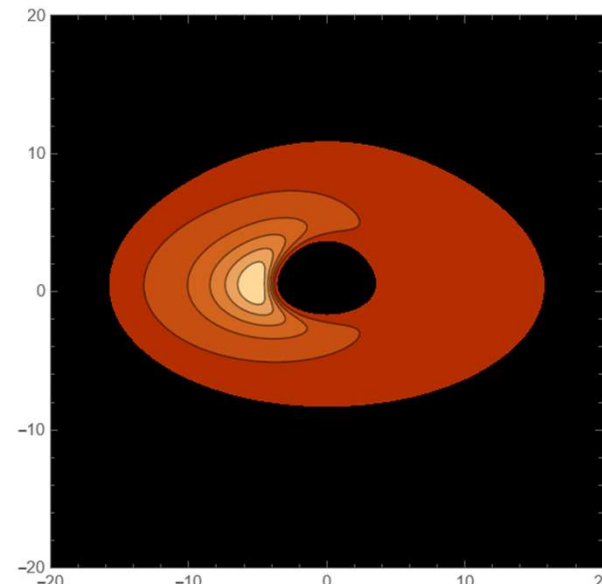
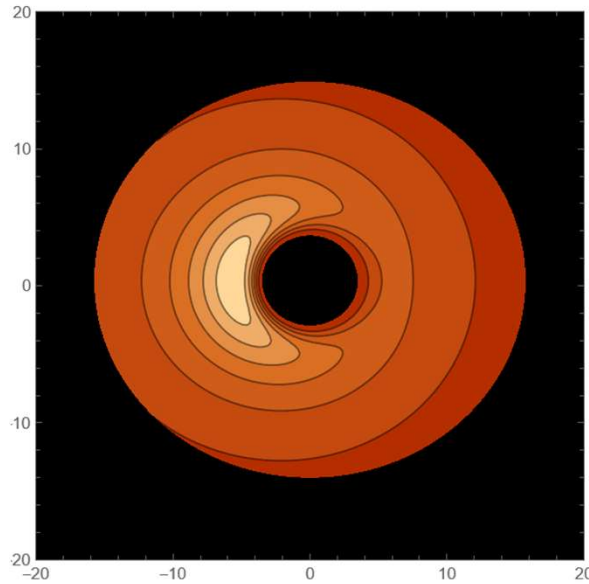
$$E_{em} = p_t \mu^t + p_\varphi \mu^\varphi = p_t \mu^t \left(1 + \Omega \frac{p_\varphi}{p_t}\right)$$

$$1 + z = \frac{E_{em}}{E_{obs}} = \frac{(1 + b\Omega \sin \theta_0 \sin \alpha)}{\sqrt{-g_{tt} - \Omega^2 g_{\varphi\varphi}}}$$

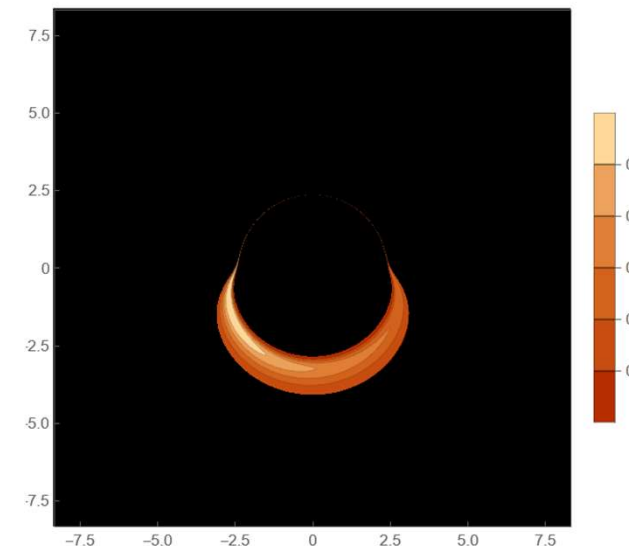
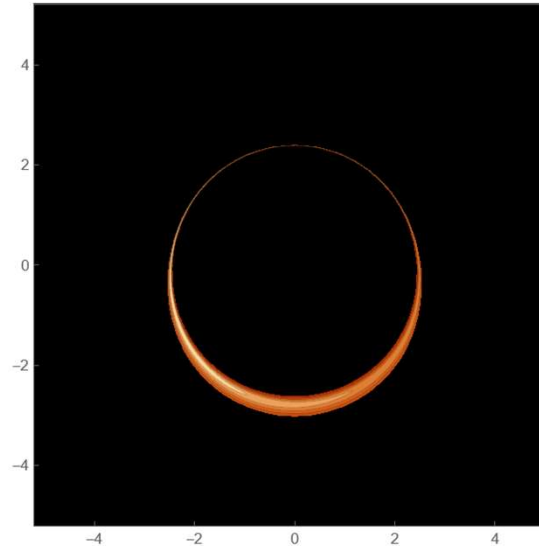
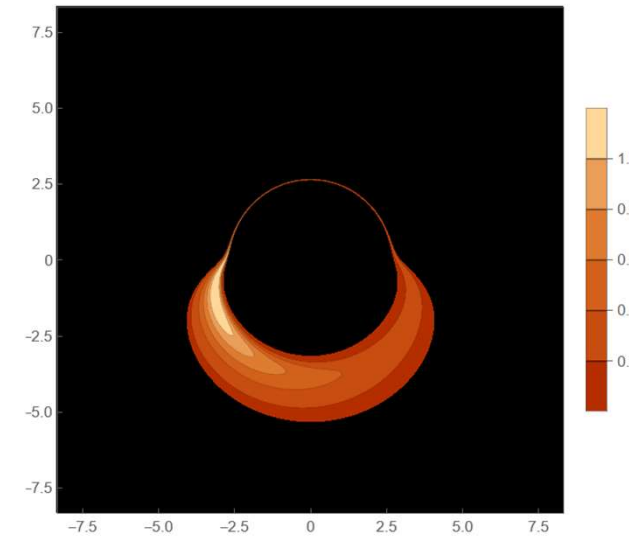
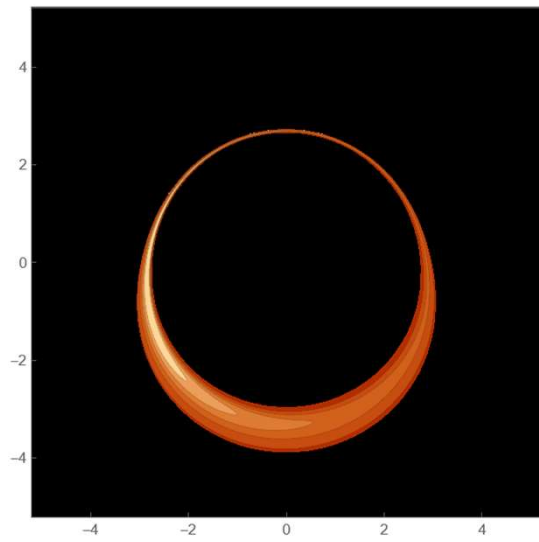


三、吸积盘的光线追踪与辐射通量

观测通量分布



三、吸积盘的光线追踪与辐射通量





- 高阶导数引力理论下的球对称黑洞解
- 黑洞时空中的测地线与光线追踪
- 薄吸积盘的观测辐射通量
- 结论

四、总结

- 1、高阶导数引力下视界为2、3的非史瓦西黑洞没有稳定的圆轨道，另外这两种时空下在 $h'(r) < 0$ 时，黑洞可能表现为排斥粒子。
- 2、视界为1时，非史瓦西黑洞薄吸积盘的主要图像与史瓦西黑洞相差不大，非史瓦西黑洞的次级图像比史瓦西黑洞更加紧凑。
- 3、非史瓦西黑洞的本征辐射通量，红移分布，与观测通量分布整体小于史瓦西黑洞，但分布规律与史瓦西黑洞相差无几，观测倾角越大，红移现象越明显。

主要参考文献

- [1] H. Lu, A. Perkins, C.N. Pope, K.S. Stelle, Phys. Rev. Lett. 114, 171601 (2015).
- [2] J.-P. Luminet, Image of a spherical black hole with thin accretion disk, Astron. Astrophys. 75, 1 (1979).
- [3] K. Akiyama et al. [Event Horizon Telescope Collaboration], Astrophys. J. L1-L6: 875 (2019);
- [4] R. Abbott et al, [LIGO Scientific Collaboration, Virgo Collaboration, and KAGRA Collaboration], Observation of Gravitational Waves from a Binary Black Hole Merger, Phys. Rev. Lett. 116: 061102, (2016).



地球物理与空间信息学院
School of Geophysics and Geomatics

谢谢